

ADA 047355

AFAPL-TR-77-62

(P2)
B-5

PERFORMANCE EVALUATION OF A CATALYTIC PARTIAL OXIDATION HYDROGEN GENERATOR USING TURBINE ENGINE FUELS

JET PROPULSION LABORATORY
CALIFORNIA INSTITUTE OF TECHNOLOGY
PASADENA, CALIFORNIA 91103

OCTOBER 1977

TECHNICAL REPORT AFAPL-TR-77-62
Final Report for Period 1 October 1976 – 30 April 1977

FILE COPY

Approved for public release; distribution unlimited.

AIR FORCE AERO PROPULSION LABORATORY
AIR FORCE SYSTEMS COMMAND
UNITED STATES AIR FORCE
WRIGHT-PATTERSON AFB, OHIO 45433

D D C
REF ID: A65142
DEC 8 1977
REGISTRATION
D

NOTICE

When Government drawings, specifications, or other data are used for any purpose other than in connection with a definitely related Government procurement operation, the United States Government thereby incurs no responsibility nor any obligation whatsoever; and the fact that the government may have formulated, furnished, or in any way supplied the said drawings, specifications, or other data, is not to be regarded by implication or otherwise as in any manner licensing the holder or any other person or corporation, or conveying any rights or permission to manufacture, use, or sell any patented invention that may in any way be related thereto.

This report has been reviewed by the Information Office (OI) and is releasable to the National Technical Information Service (NTIS). At NTIS, it will be available to the general public, including foreign nations.

This program was funded with FY76 Aero-Propulsion Laboratory Director's Funds.

This technical report has been reviewed and is approved for publication.

Leonard C. Angello
Project Engineer

FOR THE COMMANDER

Arthur V. Churchill
ARTHUR V. CHURCHILL
Chief, Fuels Branch
Fuels and Lubrication Division

"If your address has changed, if you wish to be removed from our mailing list, or if the addressee is no longer employed by your organization please notify AFAPL/SFF, W-PAFB, OH 45433 to help us maintain a current mailing list".

Copies of this report should not be returned unless return is required by security considerations, contractual obligations, or notice on a specific document.

UNCLASSIFIED

SECURITY CLASSIFICATION OF THIS PAGE (When Data Entered)

DD FORM 1 JAN 73 1473 EDITION OF 1 NOV 68 IS OBSOLETE

UNCLASSIFIED

SECURITY CLASSIFICATION OF THIS PAGE (When Data Entered)

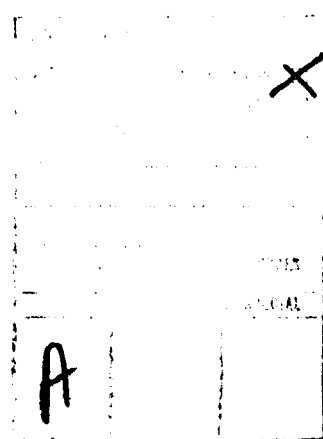
UNCLASSIFIED

SECURITY CLASSIFICATION OF THIS PAGE(When Data Entered)

20. Abstract (Con't)

The concept of using the very fuel-rich partial oxidation process as a first stage of a two-stage combustion system for onboard processing of broadened specification fuels to improve their combustion characteristics is discussed.

For the nonoptimal reactor design used, excessive catalyst bed temperatures and a propensity for solid carbon deposition in the bed were observed. These phenomena are not fully understood and need further elucidation. Thermal reactor schemes (without catalysts) may be more advantageously applied to aviation turbine engines but these schemes also require additional investigation to delineate design requirements.



D D C
REF ID: A6700000000000000000000000000000
DLG 8 1977
UNCLASSIFIED
D

UNCLASSIFIED

SECURITY CLASSIFICATION OF THIS PAGE(When Data Entered)

PREFACE

The work described in this report was performed by the Control and Energy Conversion Division of the Jet Propulsion Laboratory. The effort was supported by the Air Force Aero Propulsion Laboratory, Wright-Patterson Air Force Base, Ohio, under MIPR FY14557-601611, Project 3048, Task 304805, and Work Unit 30480582. The AFAPL project engineer was Mr. L. C. Angello, Fuels Branch, Fuels and Lubrication Division, Code AFAPL/SFF. The JPL principal investigator was Mr. R. M. Clayton.

The basic concept of onboard H₂ generation using the partial oxidation process and the two-stage combustion system incorporating it, the generator design technology, and the test facilities, all as described herein, were developed under previous sponsorship of the Aeronautical Propulsion Division, Office of Aeronautics and Space Technology. NASA, Washington, DC.

The author expresses special acknowledgment of Donald Cerini who was the principal designer of the baseline H₂ generator; this generator has recently been successfully operated in flight, supplying generator product gases to a general aviation piston engine aircraft. He was also the principal designer for the modified version of that generator used in the present work and the chief consultant in the operation of the generator in these experiments.

The initiative and interest of Roy Bjorklund, test engineer, and Clarence Tuttle, engineering assistant and facility operator, are also gratefully appreciated.

TABLE OF CONTENTS

	<u>Page</u>
I. INTRODUCTION	1
II. THEORETICAL CONSIDERATIONS	2
A. Partial Oxidation Products	2
B. Integrated Combustion System	3
III. DESCRIPTION OF EXPERIMENTS	4
A. Generator	4
B. Test Setup	5
C. Instrumentation	6
D. Fuels	7
E. Procedure	7
IV. RESULTS AND DISCUSSION	8
A. Product Gas Composition	9
B. Solid Carbon Formation and Bed Temperature Distribution . . .	10
V. CONCLUSIONS AND RECOMMENDATIONS	12
REFERENCES	14

LIST OF ILLUSTRATIONS

	<u>Page</u>
1. Theoretical Equilibrium Composition and Temperature-Idle Condition	15
2. Theoretical Equilibrium Composition and Temperature-Cruise Condition	16
3. Theoretical Equilibrium Composition and Temperature-Maximum Power Condition	17
4. Theoretical Hydrogen to Fuel Mass Ratio for Various Power Conditions	18
5. Schematic of Two-Stage Combustion System	19
6. Conceptual Operating Map for 2-Stage Combustion System	20
7. Variation of Air Split for all Fuel Through 1st Stage	20
8. Variation of Final Reaction Equivalence Ratio with Air Used for Cooling and Dilution	21
9. Schematic of Generator L	22
10. Generator L: Disassembled and Assembled	23
11. Schematic of Generator L Test Setup in High Pressure Combustion Facility	24
12. Generator L Test Installation	25
13. Product Compositions for Generator L	26
14. Hydrogen Yield Indices for Generator L	27
15. Axial Profiles of Bed Temperatures for Generator L	28
16. Overall Pressure Drop Characteristics for Generator L during Operation	29
17. Calculated Solid Carbon Production for Generator L	30

LIST OF TABLES

	<u>Page</u>
1. Comparison of Two-Stage Operational Schemes	31
2. Measurement Description	32
3. Tabulated Results	34

I. INTRODUCTION

Recent large price increases for aircraft turbine engine fuels and possible future fuel shortages have led to increased interest in widening the spectrum of fuels (including those from coal and oil shale syncrudes) acceptable for aviation turbine engine operation. It is expected that a broader spectrum of acceptable fuels would lead to substantial fuel cost savings in the total life cycle costs of operating those engines.

A potential means of accomplishing this is the concept of onboard fuel processing which, in principle, has the effect of decoupling the properties of the raw turbine fuel from the main combustion processes of the engine. The process of present interest is partial oxidation where a large portion of the fuel to the engine would be reacted with a small portion of the air to the engine in a precombustion stage of an overall two-stage combustion system. Such a processing stage would emit a stream of gaseous products whose composition is dependent on the fuel richness of the reaction and on the hydrogen content of the fuel.

With fuels having hydrogen to carbon ratios of approximately 1.9, air to fuel ratios in the range of 5-6 theoretically produce a gas stream consisting of over 20% by volume of both H₂ and CO, the remainder of the products consisting mainly of N₂. A "fuel gas" of this composition exhibits superior combustion characteristics to those of the initial raw hydrocarbon fuel by virtue of: (1) its H₂ content providing a reduced lean flammability limit, (2) its fully gaseous state, and (3) potentially reduced radiant emission.

It is envisioned that ultimately this processing stage could be physically integrated with the combustor. The partial oxidation products would then be directed into the combustor where they would be mixed with additional air, and any remaining fuel, and burned in the combustor.

Essentially the same concept (known as H₂-enrichment) is under investigation at JPL under NASA sponsorship for other applications. These include fuel economy improvement for aircraft piston engines and emission reduction for gas turbine engines. Therefore, a certain level of technology existed that provided background and encouragement for extending application of the concept to the Air Force interest in broadened specification fuels. The work reported herein was undertaken as a companion effort to the ongoing research on turbine combustion emission reduction.

The present effort was an experimental program that initiated the exploration of feasibility of onboard hydrogen generation from aviation turbine fuel. The work accomplished comprised: (1) design modifications to an existing baseline H₂-generator design (catalytic) available from the NASA program on aircraft piston engines; (2) fabrication of the revised generator and necessary test components; (3) experimental characterization of the steady state performance of the revised generator with inlet air temperature and pressure simulating an idle power condition, approximately 3 atm at 300°F, using JP5 fuel and a blend of JP5 and xylene (C₈H₁₀).

It was not intended that the baseline generator as revised would be an optimum design concept for turbine engine application. Neither was it intended

that this effort would establish such an optimum design. Rather, it was intended that use of the baseline design as revised would provide an expeditious first step in extending the application of onboard H₂ generation to aviation gas turbine engines.

It was also planned to operate the generator with inlet air state conditions simulating cruise and maximum power levels typical for Air Force aviation turbine engine operation; 8 atm of 830°F and 25 atm of 940°F, respectively. But experimental difficulties with high catalyst temperatures and soot deposition observed at the idle power level precluded operation at those more severe conditions.

II. THEORETICAL CONSIDERATIONS

A. Partial Oxidation Products

Although the partial oxidation process can be carried out either thermally or catalytically, the theoretical adiabatic equilibrium composition of the product gases are identical for the same initial reaction conditions. Details of the paths of the combustion chemistry for either reaction scheme are complex and not fully understood and their discussion is beyond the scope of this report. Suffice to say that the overall process occurs with an excess of fuel and that the consumption of the available oxygen by a portion of the fuel provides heat, CO₂ and H₂O that react with the remainder of the fuel to produce a final product gas whose composition is a function of the particular fuel stock and the reaction mixture ratio.

Figures 1-3 show the results of one-dimensional equilibrium thermochemical calculations giving product compositions (molar basis) and temperatures for a typical conventional turbine fuel with a hydrogen to carbon ratio of 1.92, over a range of fuel-rich air to fuel ratios and at the three operating conditions of interest to the present work. (Nitrogen concentrations are not shown.) The calculations were made using the computer program described in Ref. 1.

Note that solid carbon (C_s) is predicted with A/F ratios less than about 5.2 and that the product gas temperature increases rapidly at A/F ratios greater than 5.2. Carbon monoxide, one of the two major combustibles in the product gas, reaches a peak at about this A/F ratio, whereas the other major combustible, H₂, shows an increasing volumetric concentration in the A/F region of C_s formation. However, in terms of the mass of H₂ produced per unit mass of hydrocarbon fuel, it can be shown that H₂ mass productivity of the fuel also peaks at about the A/F ratio of 5.2, as illustrated in Fig. 4.

Thus, from a theoretical standpoint, the optimal A/F ratio for sootless H₂ production is about 5.2, where the H₂ content of the product gas is about 6.3% of the mass of the combustibles in the gas. The lean flammability limit of the total product gas when mixed with additional air is estimated to occur at an overall A/F ratio of about 57 based on the procedure for fuel gas mixtures (at ambient temperature) outlined in Ref. 2, taking the H₂, CO, and CH₄ as combustibles and the H₂O, CO₂, and N₂ as inert. The substantially reduced lean limit of 57 for the product gas compared to about 24 for turbine fuels is of course the central argument for the subject concept.

B. Integrated Combustion System

Assuming that the technology for providing an optimized partial oxidation reaction existed, integrating it into a two-stage combustion system has a substantial impact on present combustor design practices. However, a rudimentary conceptual design analysis serves to outline projected operational requirements and identifies potential design options that could accommodate the broad combustion range needed for aviation gas turbine engines.

A two-stage combustion system is schematically depicted in Fig. 5 where the various fuel and air flows are also identified. It is assumed that the precombustion stage is to be operated at its optimal A/F ratio of 5.2. The basic operational and control consideration is how the total system flows should be split between the two stages. For present purposes, the fuel and air splits are defined as $\dot{m}_{fg}/\dot{m}_{ft}$ and $\dot{m}_{ag}/\dot{m}_{at}$, respectively. From these definitions and the constant mixture ratio constraint for the first stage, it can be shown that the required fuel split to the first stage is related to the overall system F/A equivalence ratio (based on $\dot{m}_{ft}/\dot{m}_{at}$) as shown by the straight lines and the right hand ordinate in Fig. 6. Each line represents an arbitrarily selected constant value of air split to the first stage. For a particular total air flow to the combustion system (i.e., a particular engine power level), each of these lines also represents a constant total throughput for the precombustion stage.

If all the system fuel is directed through the first stage then operation of the combustion system lies along the abscissa and the air split no longer can remain constant. The required air split for all fuel through the first stage is shown as a function of system equivalence ratio in Fig. 7.

The curved line shown on Fig. 6 is an estimated lean limit line based on considering the first stage product gas stream as a fuel gas mixture having a composition and lean limit specified from the theoretical calculations discussed above. When all the raw fuel is processed through the first stage, this fuel gas mixture is the only "fuel" burned in the second stage, therefore the system lean flammability limit is at its minimum value. When lesser amounts of raw fuel are processed (fuel split ratios < 100%), the system lean limit increases by virtue of the increased lean limit of the raw fuel that bypasses the first stage and enters the combustion process in the second stage without prior processing.

The lean limit line represents a theoretical combustion limit, but not necessarily a lean blowout limit, since blowout is also a function of flame stabilization technique and reaction premixedness. Nevertheless, all other combustor factors fixed, fuels or fuel mixes with substantially lower flammability limits can be expected to provide substantially leaner blowout limit.

If the final combustion is to be carried out totally premixed with all the air to the second stage ($\dot{m}_{ad} = 0$), then only the system equivalence ratio region to the right of the limit line, shown in Fig. 6, is theoretically viable for completing the combustion reaction started in the precombustion stage. If a portion of the total air flow is to be used for film-cooling and dilution ($\dot{m}_{ad} > 0$) as would be required for an engine combustor, the final combustion reaction would necessarily be richer and the overall equivalence ratio could lie to left of the limit line so long as the final reaction equivalence ratio was to the right of

the limit line. The final reaction equivalence ratio in that case depends on the fraction of the total system air used for cooling and dilution and the overall equivalence ratio required for a particular engine operating condition. An evaluation of this relationship is shown in Fig. 8 for overall equivalence ratios of 0.3, 0.25 and 0.15 which are typical for maximum, cruise, and idle power, respectively. For all fuel through the first stage, air fractions of 0.45 or greater would keep the final reaction equivalence ratio above the lean limit for all power conditions.

From the foregoing discussion and a further inspection of Fig. 6, four distinct schemes for system operation can be defined and are shown in Table 1. Scheme (1) would provide the greatest benefit for application to broadened specification fuels. But scheme (2) might also be used depending on how poor the fuel is and whether processing only a portion of it would be adequate. Scheme (2) would be simpler to implement because a variable fuel split control is probably easier than a variable air split control, although compressor bleed might also be needed at low power to throttle system air mass flow while maintaining combustion stability.

III. DESCRIPTION OF EXPERIMENTS

The experimental phase of the program utilized a catalytic, partial oxidation reactor designated H₂ generator L. The generator was operated in the JPL high pressure burner facility over the pressure range of 3.4 to 4.6 atm and with inlet air temperatures of approximately 300°F. Total mass flow through the generator ranged from 0.034 to 0.058 lbm/s. Aviation turbine fuel JP5 was used for the bulk of the experiments, but a blend of JP5 and xylene (C_8H_{10}) was used in the final experiment of the program to provide a fuel with a significantly increased aromatics content. In all experiments the product gas was analyzed for its H₂, CO, CO₂, and CH₄ content. In addition, measurements of the catalyst bed temperature profile and pressure drop were made.

A. Generator

Generator L is a version of a previous generator design that was intended for steady state operation with a turbocharged aircraft piston engine at essentially constant inlet air conditions of 1.4 atm at 150–300°F. Modifications to the previous design consisted of a revised induction/premixing system, including use of prevaporized fuel, and a revised inlet distribution scheme.

Both modifications were intended to provide for operation at pressures to 25 atm at inlet air temperatures to 940°F without preignition or flashback occurring in the induction system. The design criteria adopted for this purpose were to maintain a mixture residence time of 5 ms or less and a mixture velocity of at least 100 ft/s. The resulting design and fabrication details are documented in Ref. 3.

The generator is shown schematically in Fig. 9, and Fig. 10 a and b show disassembled and assembled views, respectively. Referring to Fig. 9, inlet air enters the ports (one or both as controlled by external valves), is directed around the bed liner through the helical air passage and exits from the single port opposite the inlet ports. The purpose of the two inlet ports is to permit

a variable amount of additional air preheat as the air absorbs the heat rejected by the bed. This preheat is greatest when all of the air enters the uppermost port, and least when all of the air enters the lower inlet port. In practice, the air was directed through the upper port for startup, but was changed to the lower port as the reaction stabilized at a steady state condition. Further modulation of the air split was not used in these experiments.

After leaving the preheating passages, the air is mixed with fuel vapor in the induction passage and the fuel/air mixture is ducted to the generator inlet, where the mixture is diffused into the bed through an array of 18 holes in the wall of the induction tube. The fuel vapor was introduced into the air through an array of nine holes near the end of the fuel injection tube. Final mixture temperatures were generally in the range of 550-600°F.

The premixed fuel and air enter the bed at the conical transition section which was filled with catalyst pellets, as was the cylindrical part of the generator. Reaction occurs throughout the bed and the resulting gaseous products are discharged through the duct at the top of the bed.

The catalyst used in all of the experiments was a pellet type, with pellets 0.25 in. diameter, 0.25 in. long. All catalyst material was manufactured by Girdler Division of Chemtron Corporation of Louisville, Kentucky. The bulk of the work was conducted using a catalyst loading consisting of a less reactive material in the conical section than for the cylindrical section of the generator. For this loading, approximately 2.6 lbm of G90B pellets were used in the conical section and 9.7 lbm of G90C pellets were loaded in the cylindrical section. These catalysts have 11 and 15% nickel by mass, respectively, and use an alumina substrate.

For startup, a portion of the catalyst bed was electrically preheated with a JPL fabricated heating element composed of four 36-in. long, Inconel sheathed, Nichrome wires of 0.032-in. diameter, coiled as shown in Fig. 10(a). A sheath diameter of 1/8 in. was generally used. The coils were spaced approximately 0.75 in. apart and positioned transversely across the lower end of the cylindrical portion of the bed as shown in Fig. 9. The coils were connected in electrical parallel by two 1/8 in. diameter solid Inconel rods supplied with a total of 1350 to 1600 kw of d.c. electrical power (30-32 V at 45-50a). This power range was adequate to heat the bed locally to 1000°F in about 10 minutes.

B. Test Setup

The system for operating the generator in the high pressure burner facility is shown schematically in Fig. 11. A photographic view of the generator installation prior to closing the pressure housing is shown in Fig. 12.

With reference to Fig. 11, the generator was supported inside the burner housing that served as an inlet air plenum into which metered, unvitiated hot air entered from the facility compressor plant. During generator operation about 95% of the total air supplied to the system bypassed the generator and was exhausted to atmosphere through the multiple sonic exhaust nozzles via a sub-sonic air bypass orifice located in the upstream wall of the exhaust plenum. This orifice comprised an appropriately sized annular gap surrounding the

generator exhaust duct. Thus the nominal operating pressure for the generator was set by adjusting the total air mass flow to the system until the desired generator back pressure was obtained in the exhaust plenum. The static pressure difference between the inlet and exhaust plenums, due to the total pressure loss across the air bypass orifice, was used to control the air flow through the generator.

By virtue of the high percentage of total system air passing through the exhaust plenum, the back pressure on the generator was not significantly affected by the hot product gases during generator operation. This large ratio of air-to-product gases also minimized combustion reactions in the exhaust plenum, although some reaction was detected before the product duct exit configuration was adjusted to reduce its flameholding tendency.

Air to the generator was supplied from the air plenum through a thermally insulated external circuit containing a subsonic venturi metering element and two remotely operated flow control valves. The first of these valves controlled generator air flow rate, while the second valve controlled the split of the air to the two generator inlet ports.

Metered quantities of fuel were supplied to the system from a pressurized tank, through an externally positioned vaporizer as shown in Fig. 11. Vaporization was accomplished in a length of stainless steel tubing wrapped around a cylindrical block of aluminum into which an array of electric heater cartridges was inserted. A three-way valve permitted dumping the fuel to the test cell exhaust system while a stable vaporization rate was established prior to generator startup.

This vaporizer performed adequately for steady state fuel flow but, since it was essentially a pool boiler, capacitance effects in vaporization rates were observed during fuel flow changes. Hence, it was necessary to make flow changes very gradually in order to maintain generator mixture ratio control.

The fuel was considered to be fully vaporized when the fuel vapor temperature in the fuel injection tube exceeded the nominal final boiling point for the fuel. For the pressure conditions used in these experiments, a temperature in the range of 450°F to 550°F was considered adequate.

C. Instrumentation

Data acquisition centered on a digital recording system connected to the test measurements through standard signal conditioning equipment. Real-time digital displays of any source measurement (including product gas analysis), as well as all computed mass flow rates and mixture ratio, were available in the test cell control room during test runs.

All data were recorded on digital magnetic tape at ten second intervals from commencement of bed heatup to run termination. For specific steady state operating points this recording rate was increased to one second intervals in order to delineate data points. Standard digital computer techniques were used to reduce the data from the magnetic test tapes.

Air flow rates were measured with subsonic venturi metering elements located in the main air supply line and in the generator air supply circuit. Standard ASME practices were followed in the meter design and primary measurement techniques. Fuel flow rate was measured with a turbine meter located upstream of a remotely controlled throttle valve and the fuel vaporizer.

The functional location of the salient pressure and temperature measurements are indicated in Fig. 11 and their functional description is listed in Table 2. Standard strain gage pressure transducers and thermocouple techniques were used for these measurements.

The static pressure drop across the catalyst bed was measured at three axial locations and the bed temperature distribution was measured at seven locations. The position of these measurements is shown in Fig. 11. Higher than expected local temperatures, especially in the conical section of the bed, often damaged the thermocouples there during a run; therefore indicated temperatures in this region were questionable at times.

On-line analysis of the generator product gas composition was accomplished by means of an uncooled stainless steel sample probe positioned in the product exhaust duct as shown in Fig. 11. A relatively large sample was transferred to remotely located analytical instruments via heavy-walled, stainless steel tubing about 300 ft. long, through the walls of which a low-voltage a.c. electrical current was passed to maintain approximately 300°F wall temperature. The transfer line was vented to atmosphere near the analytical instrument location after a small portion of the transferred gas sample was withdrawn by the instrument pumps. The sample was analyzed continuously on a dry volumetric basis for H₂, CO₂, CO, and total HC (as CH₄) content, using Thermal Conductivity, NDIR, and FID instruments for the respective analyses.

D. Fuels

The bulk of the experiments were conducted with military specification (Mil-T-5624J) grade JP5 fuel. However, the final run of the program was conducted with a fuel blend of the proportion 3.087 lbm JP5 to 1.000 lbm xylene (C₈H₁₀). This mix provided a fuel composed of about 35% aromatics by volume compared to the nominal 15% aromatics content of specification JP5.

E. Procedure

A typical test run was conducted as follows:

- (1) With the generator air valve closed, system supply air was brought up to approximately the desired startup value and maintained while preheat was established at 400°F to 425°F in the inlet plenum. This inlet plenum air temperature was necessary to counteract heat losses in the external generator air circuit and provide approximately 300°F generator inlet air.
- (2) As the air preheat approached the desired value, the total air flow-rate was trimmed to provide about 3 atm exhaust plenum pressure, and

the generator air control valves were adjusted for maximum regenerative preheating (upper air port) and for the desired startup flow to the generator. The generator flow control valve was then closed for later reopening to this preset position for the desired flow rate.

- (3) While air flows were being adjusted, the fuel vaporizer was energized and the fuel feed circuit from the vaporizer inlet, downstream, was preheated with a gaseous N₂ purge. During this preheating period, the fuel dump valve was cycled in order to heat the generator fuel circuit as well as the dump circuit.
- (4) Fuel flow was then brought up to the startup value and dumped to establish full vaporization temperature near the outlet of the dump line.
- (5) As the desired vaporization temperatures were approached, the catalyst bed heater was energized and data recording was commenced.
- (6) When the temperature in the heated region of the bed reached about 1000°F, the bed heater was de-energized and the preset generator air flow was started, simultaneously with diversion of the prevaporized fuel to the generator. All startups of this program were accomplished with a nominal 0.029 lbm/s air flow and an A/F ratio in the range of 5.0-5.3.
- (7) Startup reactions were indicated by rising catalyst bed temperatures and by a product composition transient to near theoretical equilibrium values as observed from on-line gas analysis.
- (8) When temperatures and gas analysis indicated stable operation at a selected generator mixture ratio, all data were recorded at one-second intervals, which specified the initial assigned data point for the run.
- (9) For operation at a near constant pressure and inlet temperature, different mixture ratios and/or generator throughputs were achieved by holding total system air flow constant and varying the generator air and fuel flow as appropriate. These changes were necessarily made slowly and new operating points were held until real-time data displays indicated steady operation, before new data points were assigned in the string of recorded data.
- (10) Most of the data reported herein is for the so-called idle inlet air condition with various mixture ratios and throughputs, and were therefore obtained as described in item 9. However, transits to somewhat higher pressures were also made by holding generator mixture ratio constant and increasing the total system air flow.

IV. RESULTS AND DISCUSSION

Eight test runs were conducted (designated runs 93 thru 100), seven with JP5 fuel and one with the JP5/xylene blend. The first two runs, 93 and 94, were considered shakedown runs to establish operational and instrumentation

procedures. Also two later runs, 97 and 98, were determined to have been faulty due to a leak of undeterminable magnitude in the generator air supply circuit. Therefore only the data for runs 95, 96, 99 and 100 will be discussed. Pertinent generator data for these runs are tabulated in Table 3.

All runs were terminated earlier than planned due to the collection of soot or coke in the catalyst bed which caused the generator pressure drop to exceed the ΔP available for generator air flow control. Those data obtained with excessive bed pressure drop are therefore also omitted in the discussion of generator performance. This includes the data tabulated for 95-7, 96-5, 99-11, 12, 13 and 100-6. This is reasonable since enough soot on the catalyst pellet surfaces to effect the bed pressure drop must also effect the catalyst activity, hence generator performance.

Generator performance measurements were obtained for operating pressures between 3.2 and 4.3 atm, with an inlet air temperature for the bulk of the data of about 300°F at four levels of total mass throughput, nominally 0.035, 0.042, 0.048, and 0.057 lbm/s. Data points taken early in each run, corresponding to the lowest throughput condition, had lower inlet air temperature but the regenerative preheat brought the inlet mixture temperature within a reasonably constant value in the 500°F to 600°F range for most runs, therefore all performance data are considered to be for a fixed inlet temperature. No specific trend of influence of the narrow pressure range was found, therefore no further distinction is made of operating pressure differences.

A. Product Gas Composition

The concentrations of the four measured species in the product gas as a function of metered generator A/F ratio is shown for the four levels of throughput and two fuels in Fig. 13. Concentrations are based on the dry, soot-free measurements of H₂, CO, CO₂ and HC (as CH₄) but have been converted to wet, soot-free volumetric concentrations using metered air flow rates and standard species balance procedures for estimation of water content. The estimated water concentrations are also shown in Fig. 13. The JP5/air theoretical equilibrium composition curves for 3 atm, 300°F air are shown for reference. Theoretical calculations for the blended fuel were not made.

Considerable data scatter is apparent, but taken as a whole the data for JP5 follows the trends for H₂ yield expected from theoretical considerations, with the yield generally within 90% of theoretical. Some reduction in H₂ yield is apparent as the throughput was increased to the highest value tested. But whether this was the result of a true bed capacity limitation or the effects of soot deposition is uncertain since, as discussed below, the highest throughput levels not only gave indication of high soot production, but also occurred late in the runs when accumulated deposits were probably already present.

The data for the run with the fuel blend shows somewhat less H₂ yield than for the JP5 fuel, but this is expected since the hydrogen content of the blend is approximately 12.8% by mass compared to the nominal 13.8% for JP5.

The trend for CO yield was also consistent with the theoretical trend and also was generally within 90% of theoretical equilibrium.

The concentration of CO_2 and unconverted hydrocarbons (as CH_4) in the product gas stream were always somewhat greater than expected from theoretical considerations. This reflects the nonequilibrium performance of the generator that are apparent in the less than theoretical yield of H_2 and CO previously mentioned.

Since the H_2 content of the product gas is considered to be the most influential factor in the concept of improving the combustion properties of the raw fuel by onboard fuel processing, the quantity of H_2 produced per unit quantity of fuel (H/F) and the fraction of H_2 in the total combustibles are important indices of generator performance. Maximizing these indices would provide the optimal application of the partial oxidation process to the two-stage concept for broadening acceptable fuel specifications. The H/F mass ratios and H_2 fraction in the combustibles observed in these tests are shown in Fig. 14 where they again compare favorably with theoretical equilibrium values. As did the volumetric H_2 yields, the H/F ratios for JP5 fuel generally fall within 90% of the theoretical values with some reduction indicated for the higher throughput levels. The fuel blend, of course, exhibits a reduced H_2 mass production due to its smaller initial hydrogen content.

In summary, the fuel gas stream produced by the catalyzed partial oxidation process, and in particular by the generator tested, using a conventional and an unconventional turbine fuel, appears to be near the theoretical gaseous composition attainable. This result is consistent with previous JPL experience using similar generators with gasoline fuels, operated at atmospheric pressure. The utility of this fuel gas stream in application to a second stage of combustion in a continuous flow turbine-engine-like burner system of course remains to be demonstrated.

B. Solid Carbon Formation and Bed Temperature Distribution

Although seemingly diverse results, the observed deposition of solid carbon in the catalyst bed and the observed excessive temperatures in the bed are believed to be interrelated and will be discussed as such, although more detailed diagnostic measurements than were possible in these experiments would be required to fully delineate the interrelation.

Past JPL experience with atmospheric pressure catalytic generators using gasoline has not shown either of these factors to be limiting problems so long as the operating mixture ratio is properly controlled.

The longitudinal temperature distribution near the axis of the bed is illustrated in Fig. 15. The upper three plots are for JP5 for three ranges of mixture ratio and the various throughput levels. The lower plot shows analogous results for the fuel blend for a single mixture ratio range. In all cases, super-equilibrium temperatures were observed over a substantial region of the bed with peak values of about 2400°F (the catalyst limit) near the junction of the conical and cylindrical sections of the generator. However, the temperature of the product gases at the generator exit only approached the theoretical values and never exceeded them.

The high bed temperatures are not really understood. However, one qualitative explanation postulates a preferential diffusion of oxygen to the surface of

the catalyst, providing an oxygen-rich reaction with the fuel, hence a high temperature at the surface of the pellets in the heat release zones. This, coupled with a higher heat transfer to the catalyst substrate than to the local gas flow and a high thermal resistance in a pelletized bed, could lead to heat storage in the pellets and high local temperatures relative to expected final product temperatures. More rigorous diagnostic measurements and analysis would be required to substantiate this explanation than was possible in the scope of this program.

Carbon deposition during runs was normally not observed to cause a progressive deterioration of generator performance; that is, the bed temperatures (though high), product gas composition and generator pressure drop would behave predictably according to the operational condition of generator throughput and mixture ratio. However, after a half to one hour operation, a relatively rapid increase in pressure drop would occur which was invariably accompanied by quickly deteriorating generator performance.

Overall pressure drop through the generator, before and after the onset of bed plugging, is illustrated as a function of total generator throughput in Fig. 16. Intermediate pressure drops across the bed were also made, but were generally too small to be accurately measured until plugging occurred. Suffice to say that when plugging occurred, these intermediate measurements showed that the major pressure drop increase occurred across the cylindrical rather than the conical portion of the bed.

The onset of plugging was fatal in the experimental setup because with an uncontrollable air flow decrease (generator air supply valve fully open) the capacitance effect in the fuel vaporizer would not permit a rapid decrease in fuel vapor flow to the generator. Thus, mixture ratio control was also lost, and increasingly rich operation would occur.

Carbon deposits in the bed after a run may have been biased by the run termination scenario just described, but to what degree is undeterminable. Nevertheless, the usual condition of the bed was:

- (1) The pellets in the region of the heater elements, especially the lower two elements, were usually coked or sooted sufficiently to form a caked mass. The richer the run the more solid was the coking in this region, which was also the highest temperature region in the bed as seen from Fig. 15.
- (2) The pellets in the conical section were generally sooted, but not caked together.
- (3) There was generally loose soot in the region downstream of the heater elements, the caking tendency decreasing toward the exit end of the bed and toward the core portion of the bed.
- (4) About 2 pellet layers near the liner walls of the entire bed (including the conical section) were generally caked and stuck to the wall.

- (5) Heavy carbon deposits (soot or coke) on pellets anywhere in the bed were usually accompanied by a migration of the nickel to the surface of the pellets in the form of a thin metallic shell which flaked off of the pellet substrate.

Because each run generally spanned a number of different operating conditions, it was not considered meaningful to determine solid carbon formation data from the accumulated amount of carbon formed during the runs by measuring the weight change in the bed. However, calculations were performed in an attempt to detect carbon formation tendency as a function of operating conditions using the measured flow rates to the generator and the measured product gas compositions. For these species balance calculations, it was assumed that any solid carbon formed was deposited in the bed and therefore that the product gas contained no free carbon. The rather scattered results of these calculations suggest that solid carbon was produced across nearly the complete operating range of the experiments, which is consistent with the operational experience.

These results are presented in Figs. 17 (a) and (b). Fig. 17 (a) shows the calculated mass ratio of solid carbon to generator fuel (C/F) as a function of A/F ratio. No consistent trend with mixture ratio is evident except for the lowest throughput level where C/F decreased from about 0.025 to essentially nil over the A/F range 5.02 to 5.5.

When the same results are plotted as a function of generator throughput, Fig. 17 (b), a more consistent trend of increasing C/F ratio with increasing throughput, is evident. The curve in Fig. 17 (b) is fitted through the arithmetical average of the results for the four throughput levels for JP5/air. Based on the trend of the averages, the C/F ratio increased about five-fold with an increase of throughput from 0.035 lbm/s to 0.057 lbm/s.

The calculated data for the blended fuel indicates a somewhat greater tendency for solid carbon formation as is also shown in Fig. 17 (a) and (b).

Given the high bed temperatures, the evidence of almost continuous carbon formation regardless of mixture ratio, and the presence of heavy coking in the highest temperature region of the bed, it is believed that thermal cracking of the fuel was the major contributor to the bed plugging difficulties in these experiments.

V. CONCLUSIONS AND RECOMMENDATIONS

The catalytic partial oxidation process can provide a product fuel gas stream of near theoretical equilibrium composition containing approximately 6% H₂ in the total combustibles using conventional specification JP5 turbine fuel. Similar performance (with slightly less H₂) can be obtained using an unconventional JPL/xylene blend with as much as 35% aromatics content. These results were demonstrated using a test rig scale H₂ generator operated with air inlet state conditions typical of engine idle power level (3.2-4.3 atm at 300°F). Commercially available nickel catalyst pellets were used.

The kerosine-type fuels exhibited a marked propensity for solid carbon formation and deposition in the catalyst bed. In addition, local bed tem-

peratures substantially above theoretical thermochemical equilibrium final gas temperatures were observed. These results are in contrast to previous JPL experience with the same basic generator design using gasoline fuels at atmospheric pressure and limited the range of operating conditions of the experiments to relatively low throughput rates at the idle condition.

Future work on catalytic partial oxidation technology for the subject application should emphasize well controlled laboratory experiments conducted with temperatures and pressures typical for turbine engine conditions. This work should have the objective of establishing a more fundamental understanding of the sooting limits of the turbine type fuels; in particular, the interaction of the molecular structure of the fuels with the catalytic process. Monolithic catalysts should be used in these studies since this configuration is essential for ultimate application to turbine combustors.

A number of practical design and operational considerations indicate that the partial oxidation reaction stage might be more advantageously applied if the process could be carried out thermally rather than catalytically. The potential benefits are simpler startup, greater durability, lack of abrasive particulates through the turbine, and perhaps a greater tolerance to soot production. While the design of such a precombustion stage is currently hampered by a lack of design criteria for an efficient, practical reactor, unpublished JPL experiments do give encouragement that a thermal reaction scheme is possible.

It is therefore highly recommended that work on thermal partial oxidation reactors be initiated with at least the same priority as further efforts on the catalytic scheme. The efforts on the thermal reaction should include analysis and critical review of existing information on very fuel-rich combustion to identify potential reactor design concepts amenable to gas turbines, laboratory verification of promising concepts, and finally, test rig scale reactor design and evaluation.

REFERENCES

1. Gerdon, S. and McBride, B. J., Computer Program for Calculation of Complex Chemical Equilibrium Compositions, Rocket Performance, Incident and Reflected Shocks, and Chapman-Jouguent Detonations, NASA SP-273, Lewis Research Center, Cleveland, Ohio, 1971.
2. Coward, H. F. and Jones, G. W., Limits of Flammability of Gases and Vapors, Bulletin 503, Bureau of Mines, Washington, D.C., 1952.
3. JPL Fabrication Drawings, D10082203 thru D10082210, Revision A (JPL internal document).

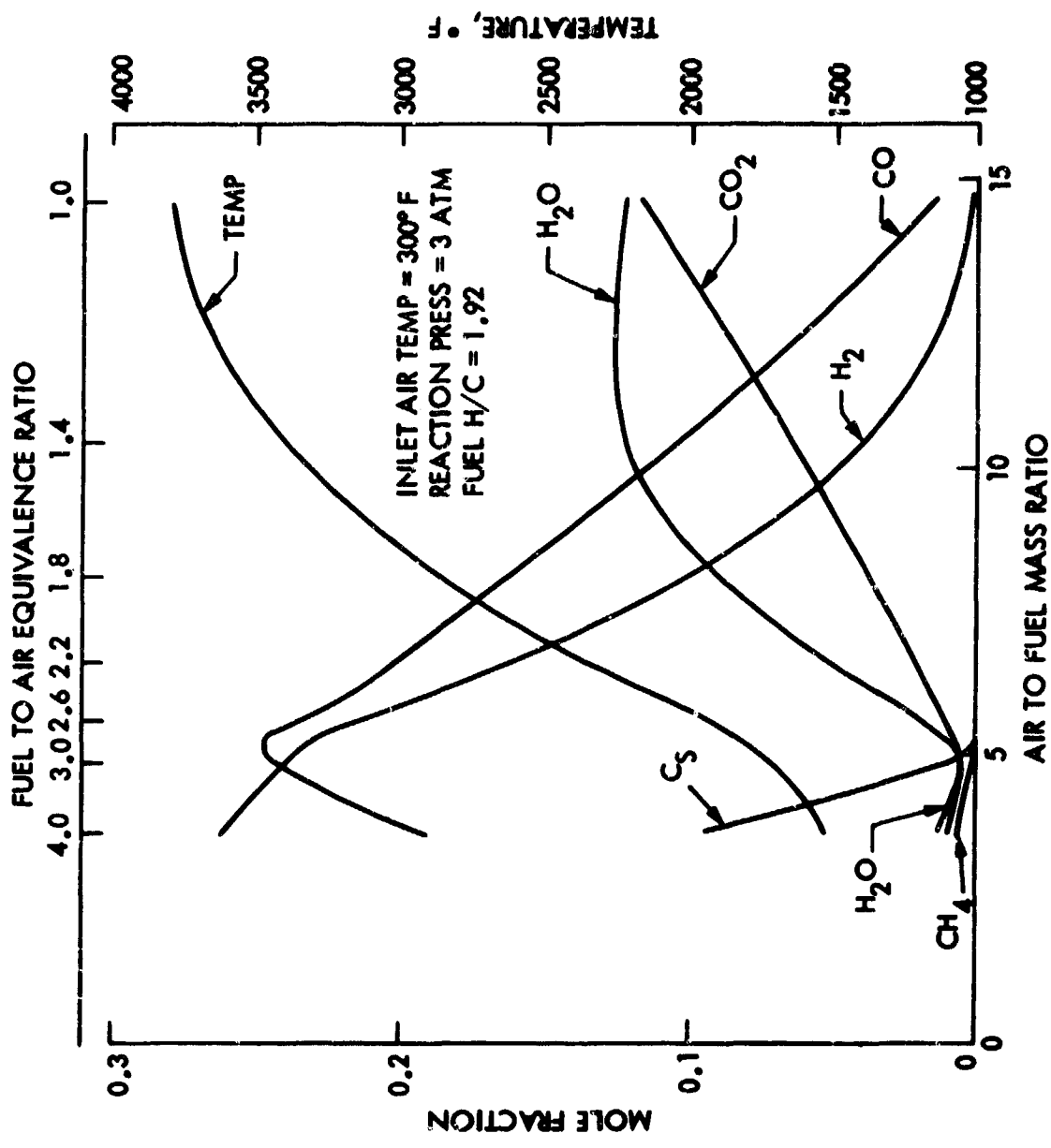


Figure 1. Theoretical Equilibrium Composition and Temperature – Idle Condition

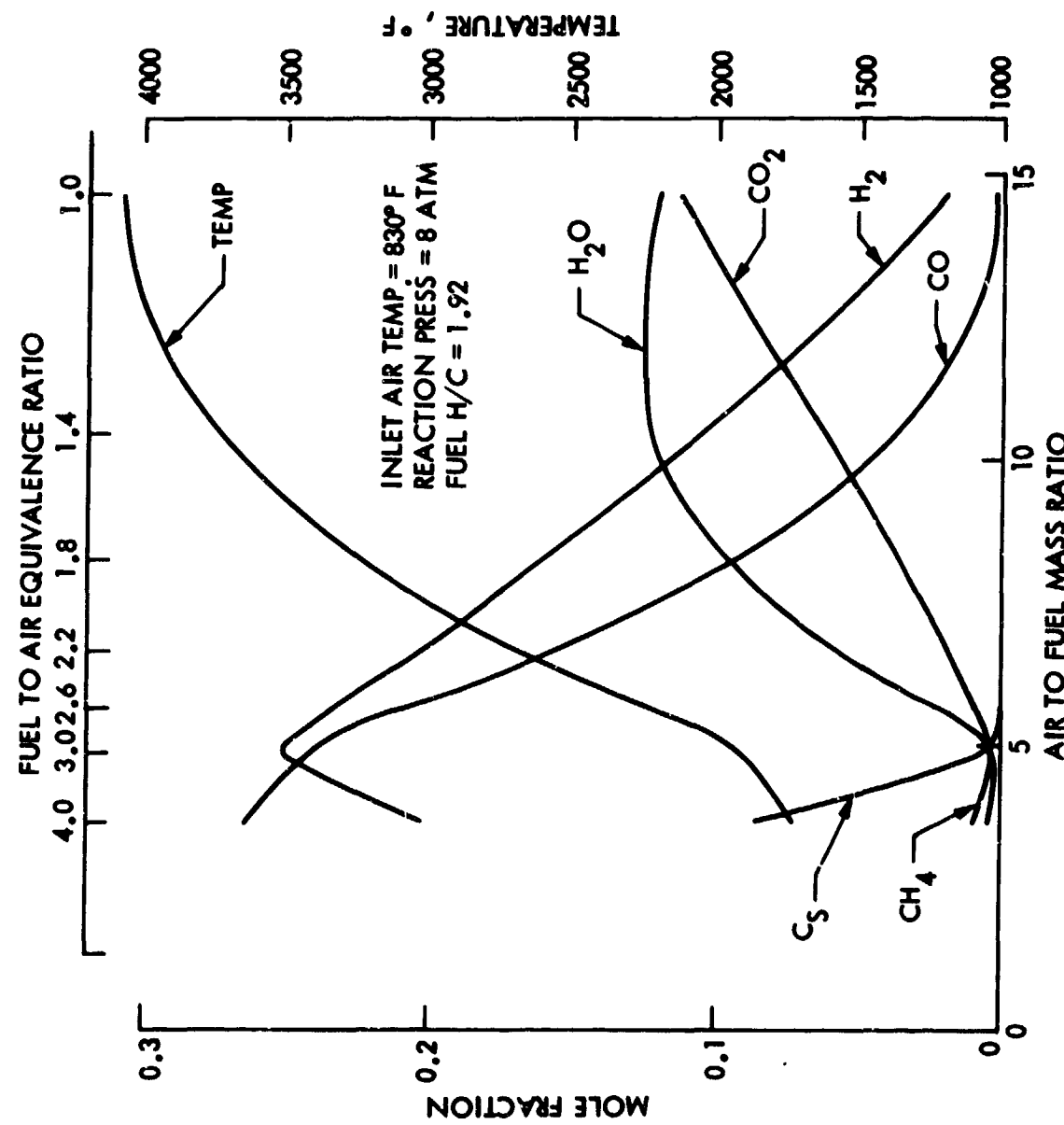


Figure 2. Theoretical Equilibrium Composition and Temperature - Cruise Condition

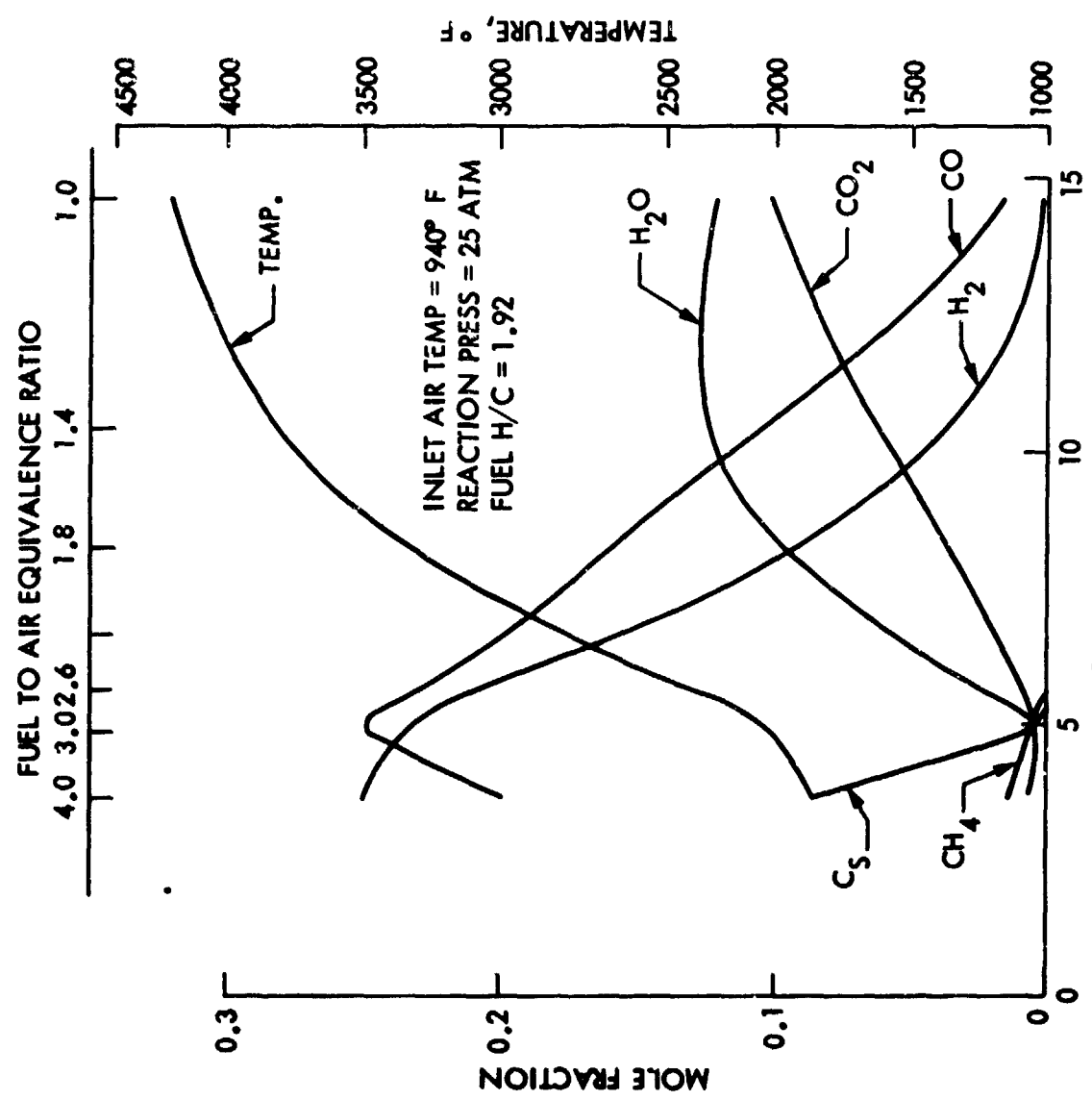


Figure 3. Theoretical Equilibrium Composition and Temperature - Maximum Power Condition

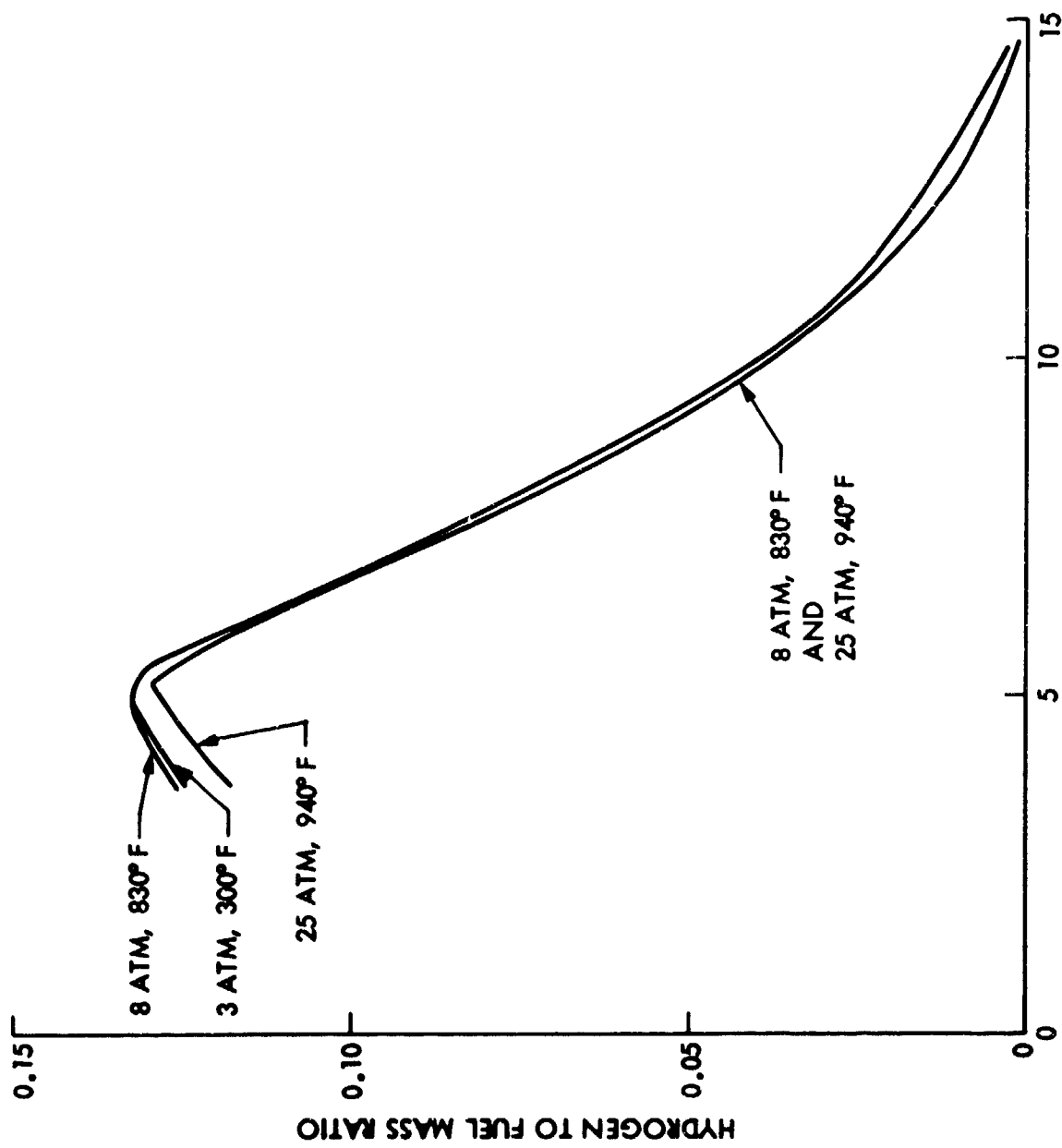


Figure 4. Theoretical Hydrogen to Fuel Mass Ratio
for Various Power Conditions

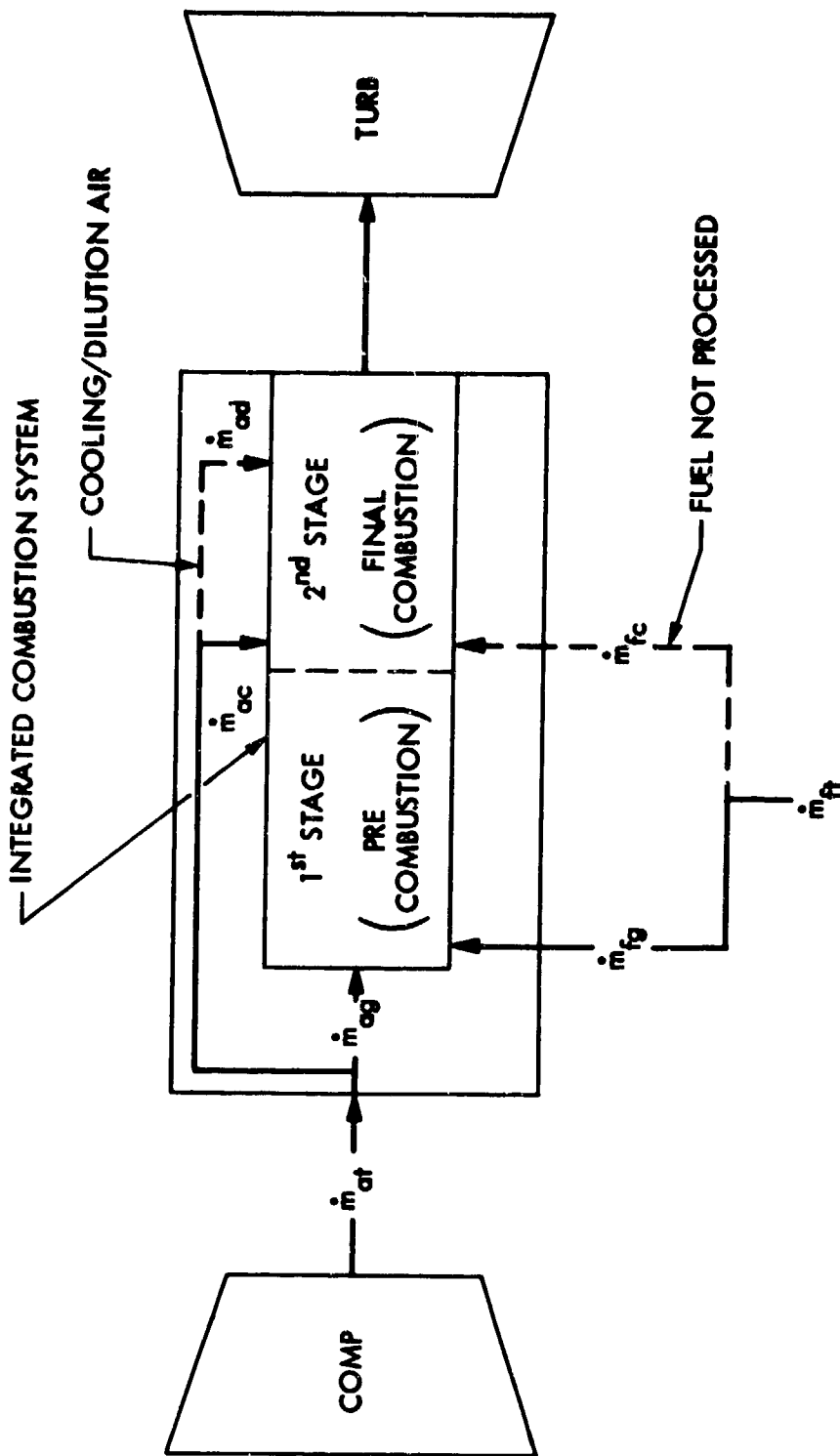


Figure 5. Schematic of Two-Stage Combustion System

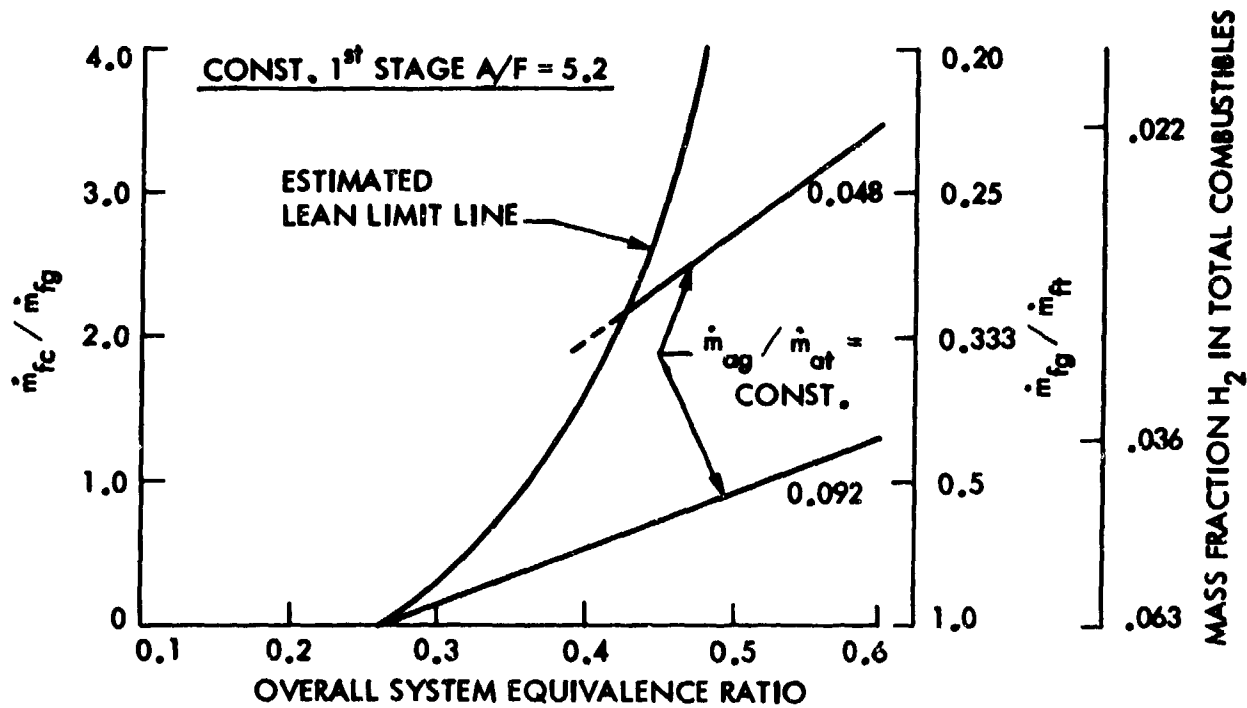


Figure 6. Conceptual Operating Map for 2-Stage Combustion System

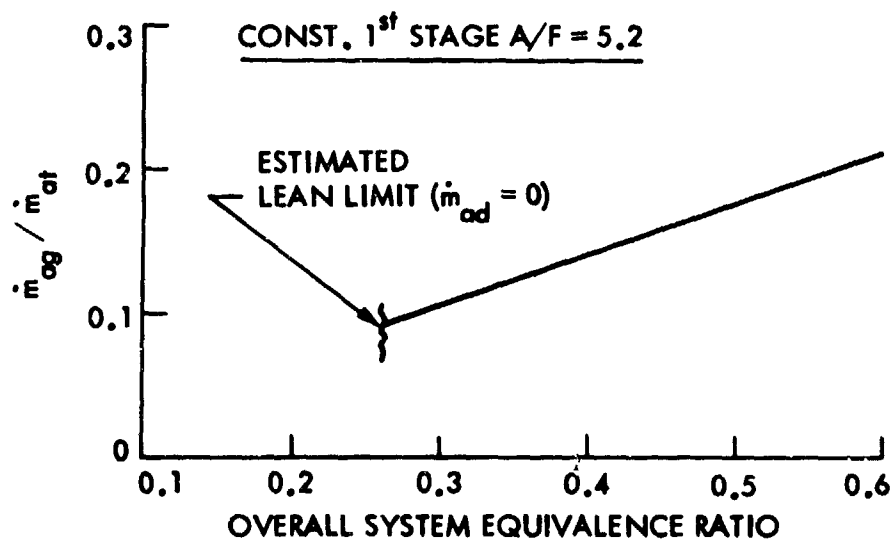


Figure 7. Variation of Air Split for All Fuel Through 1st Stage

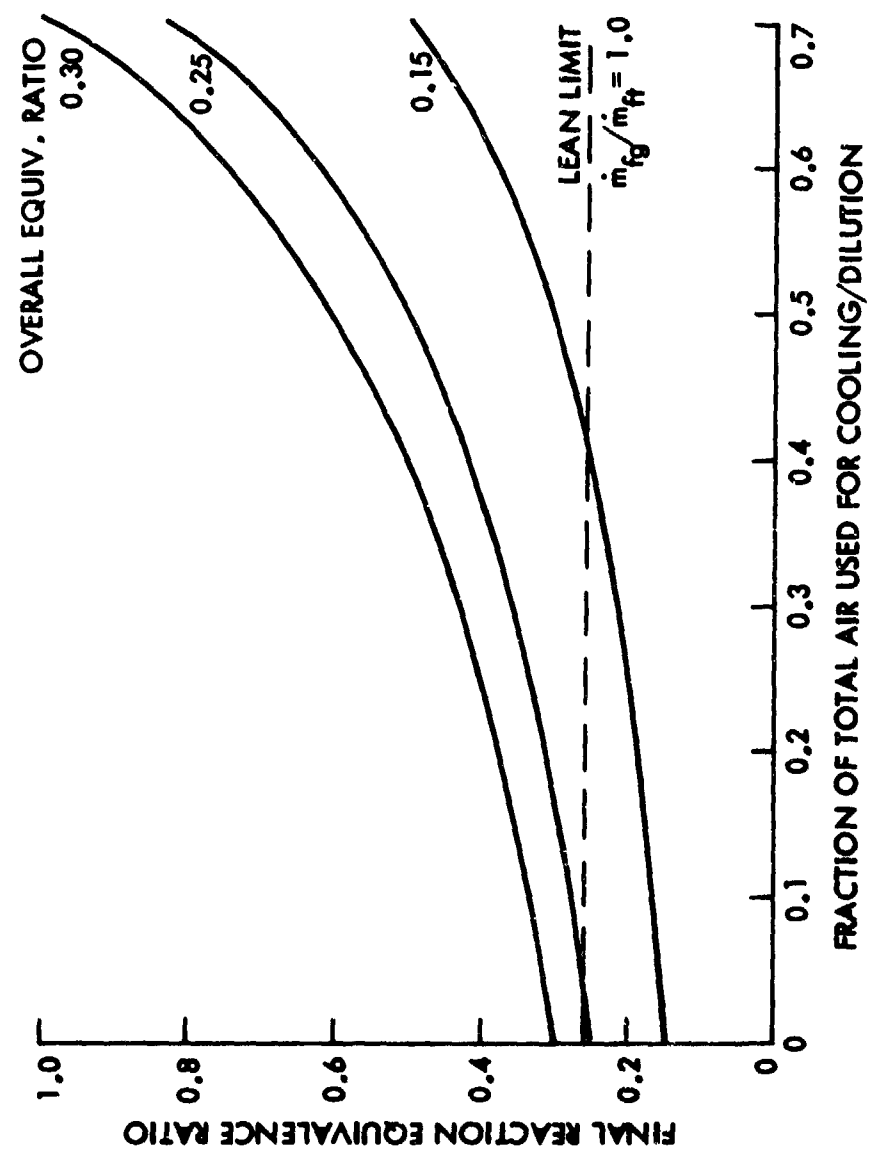


Figure 8. Variation of Final Reaction Equivalence Ratio with Air Used for Cooling and Dilution

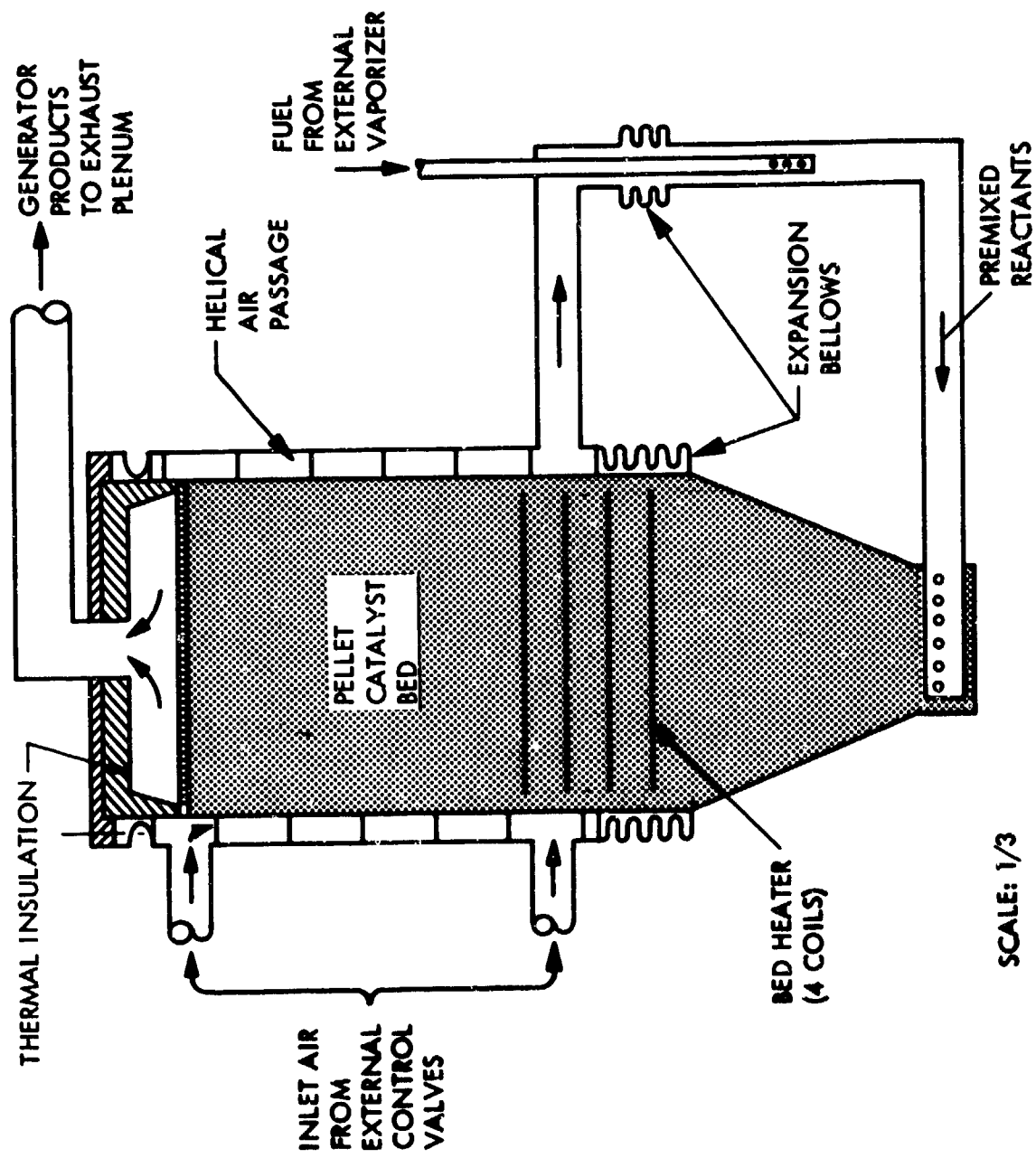


Figure 9. Schematic of Generator L

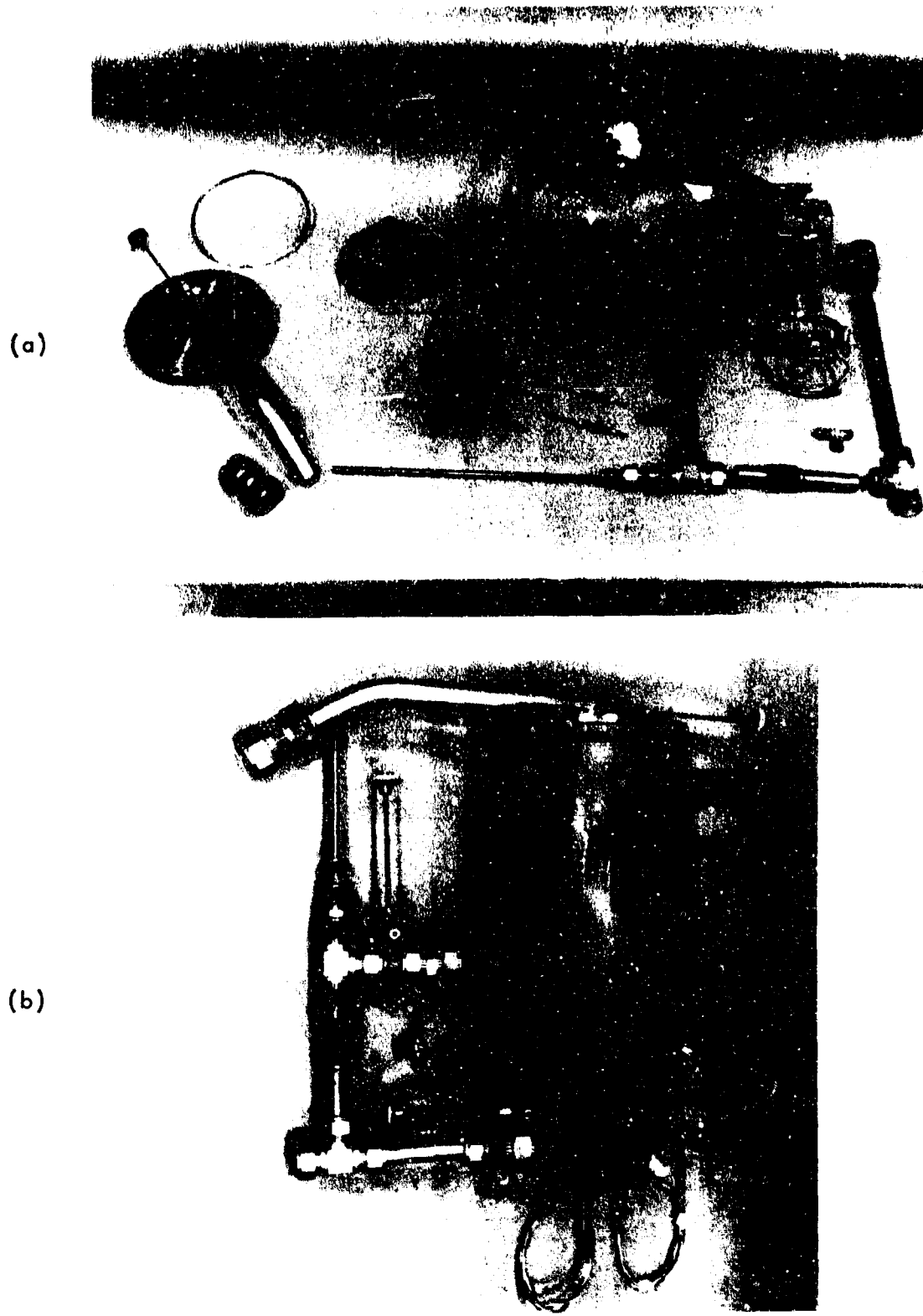


Figure 10. Generator L: (a) Disassembled; (b) Assembled

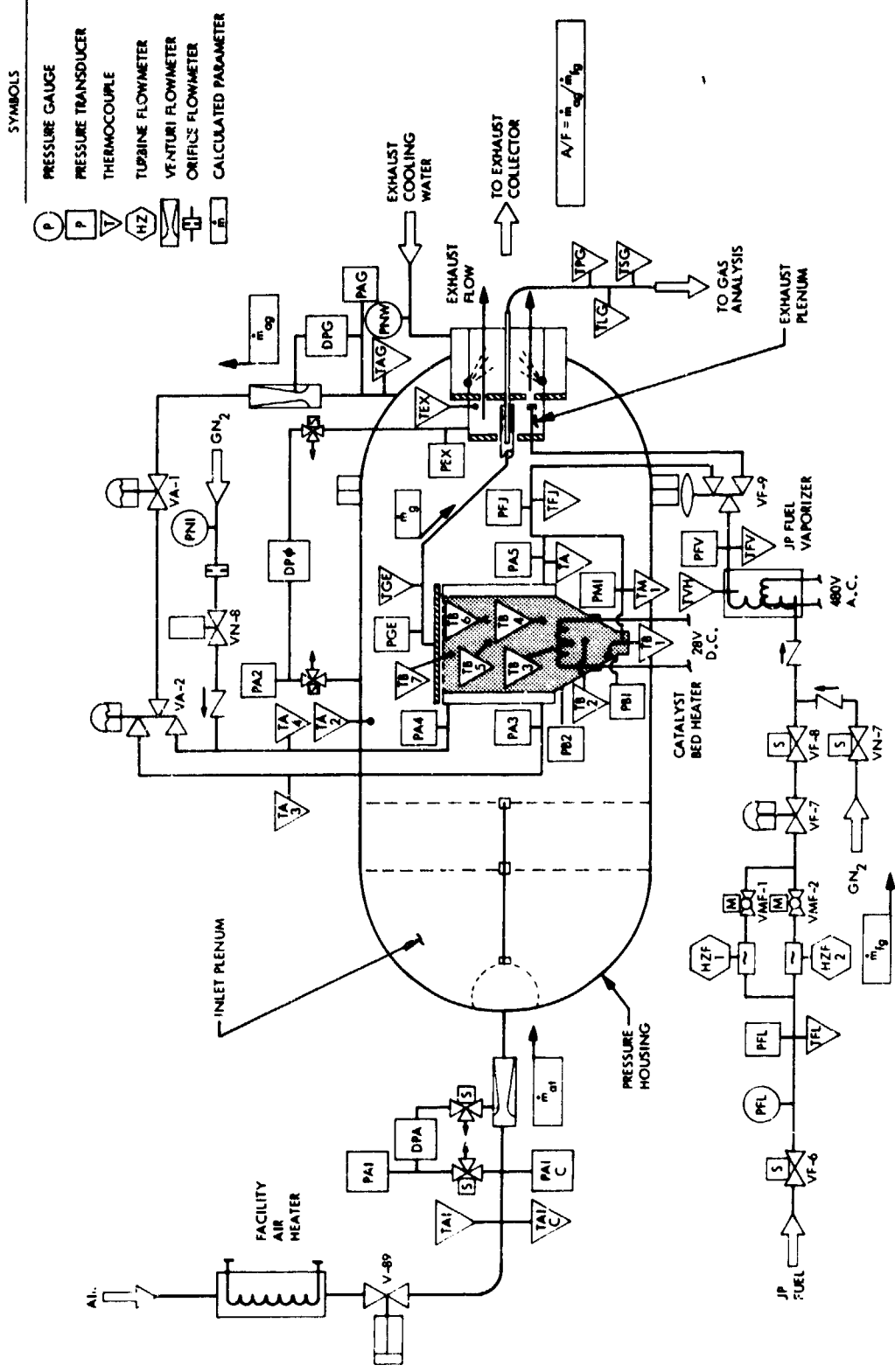




Figure 12. Generator L Test Installation

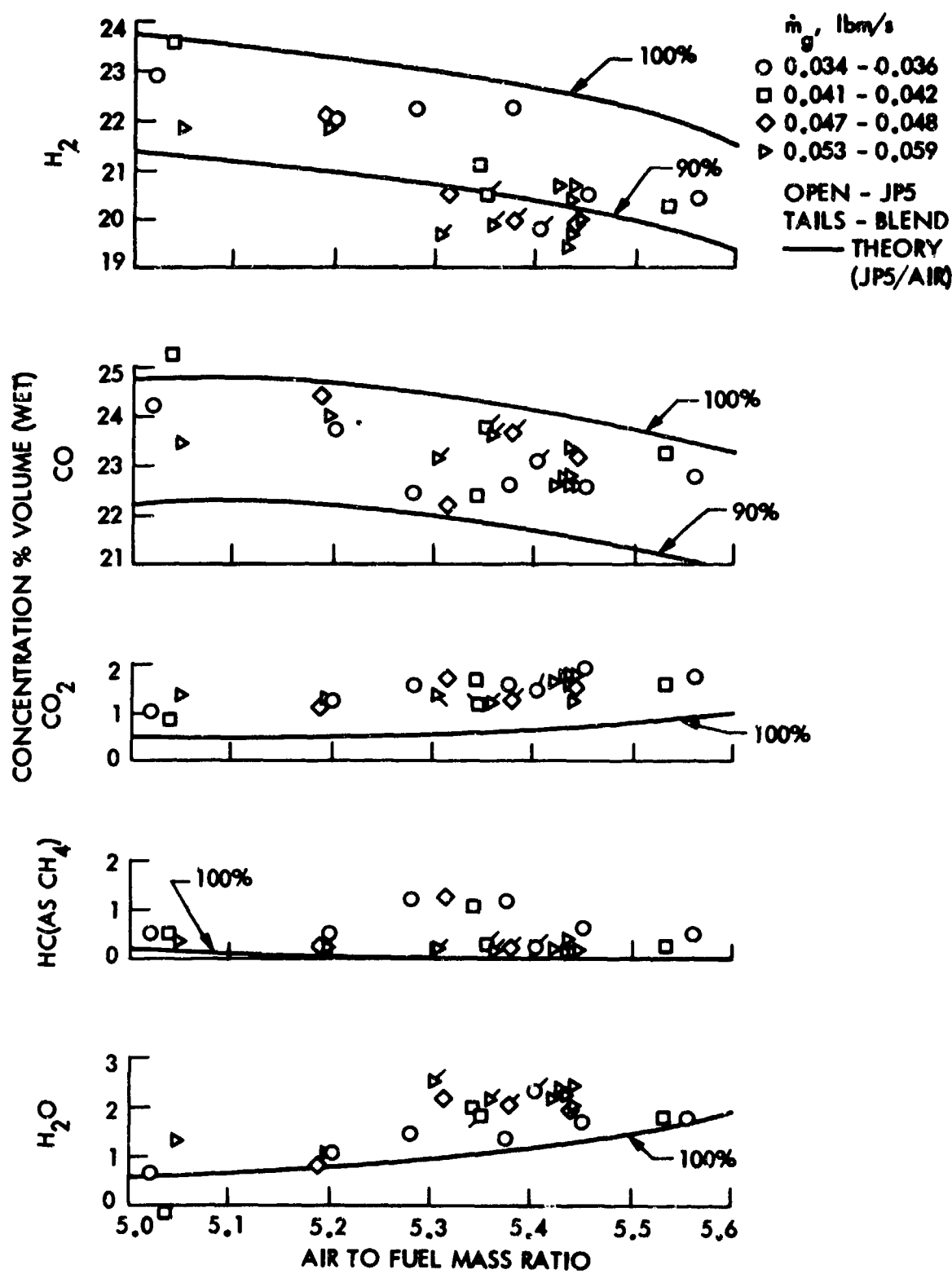


Figure 13. Product Compositions for Generator L

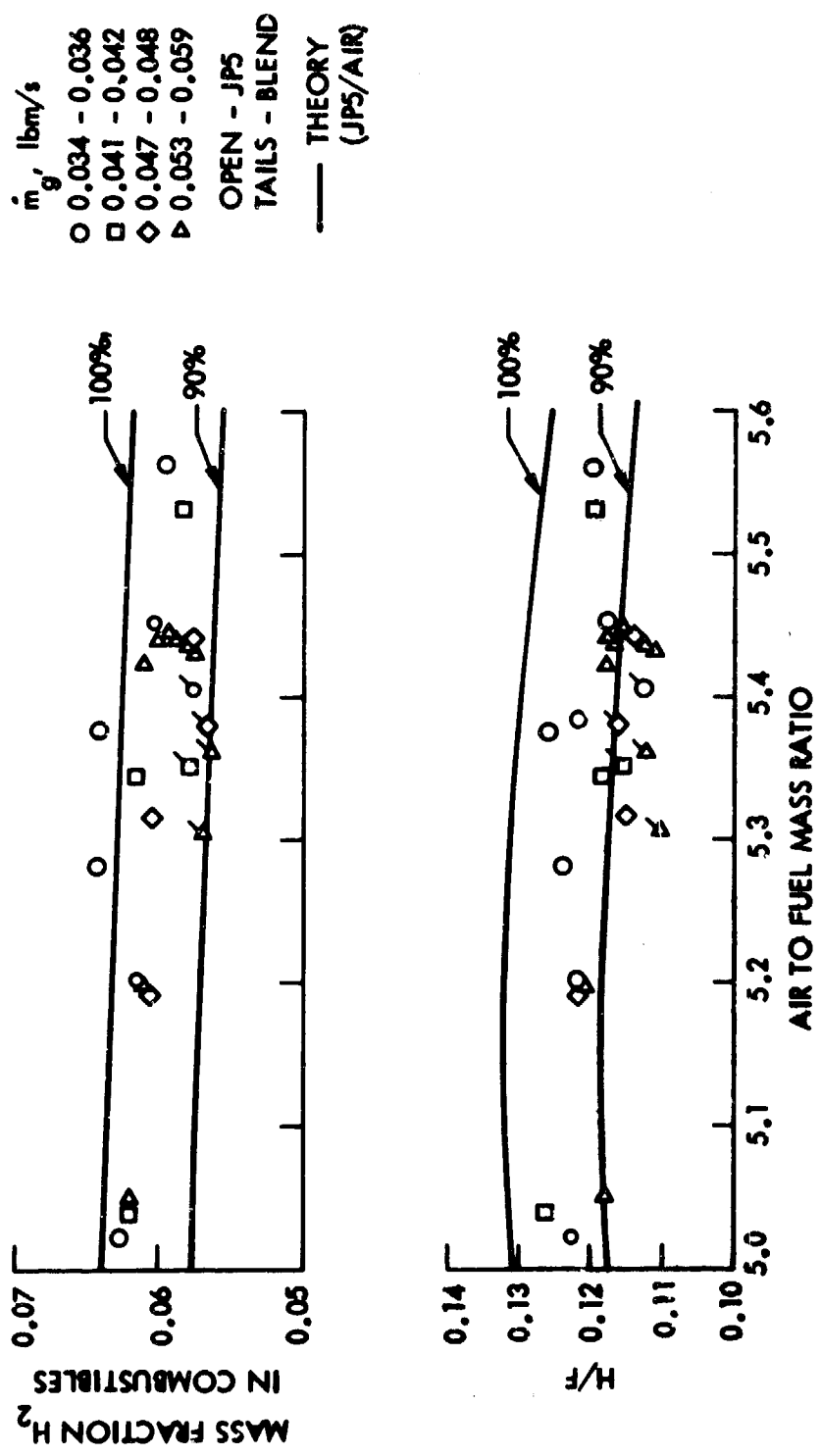


Figure 14. Hydrogen Yield Indices for Generator L

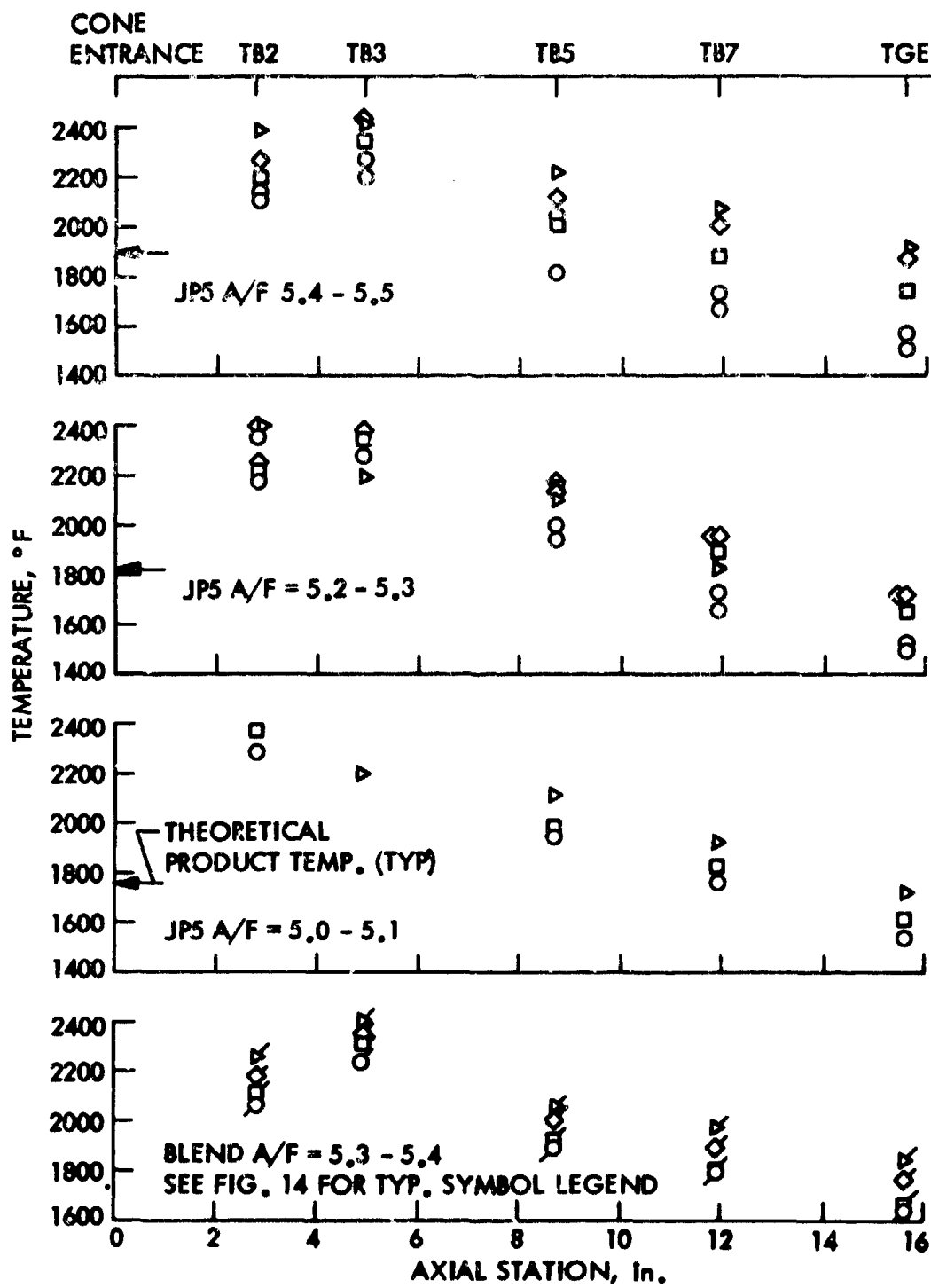


Figure 15. Axial Profiles of Bed Temperature for Generator L

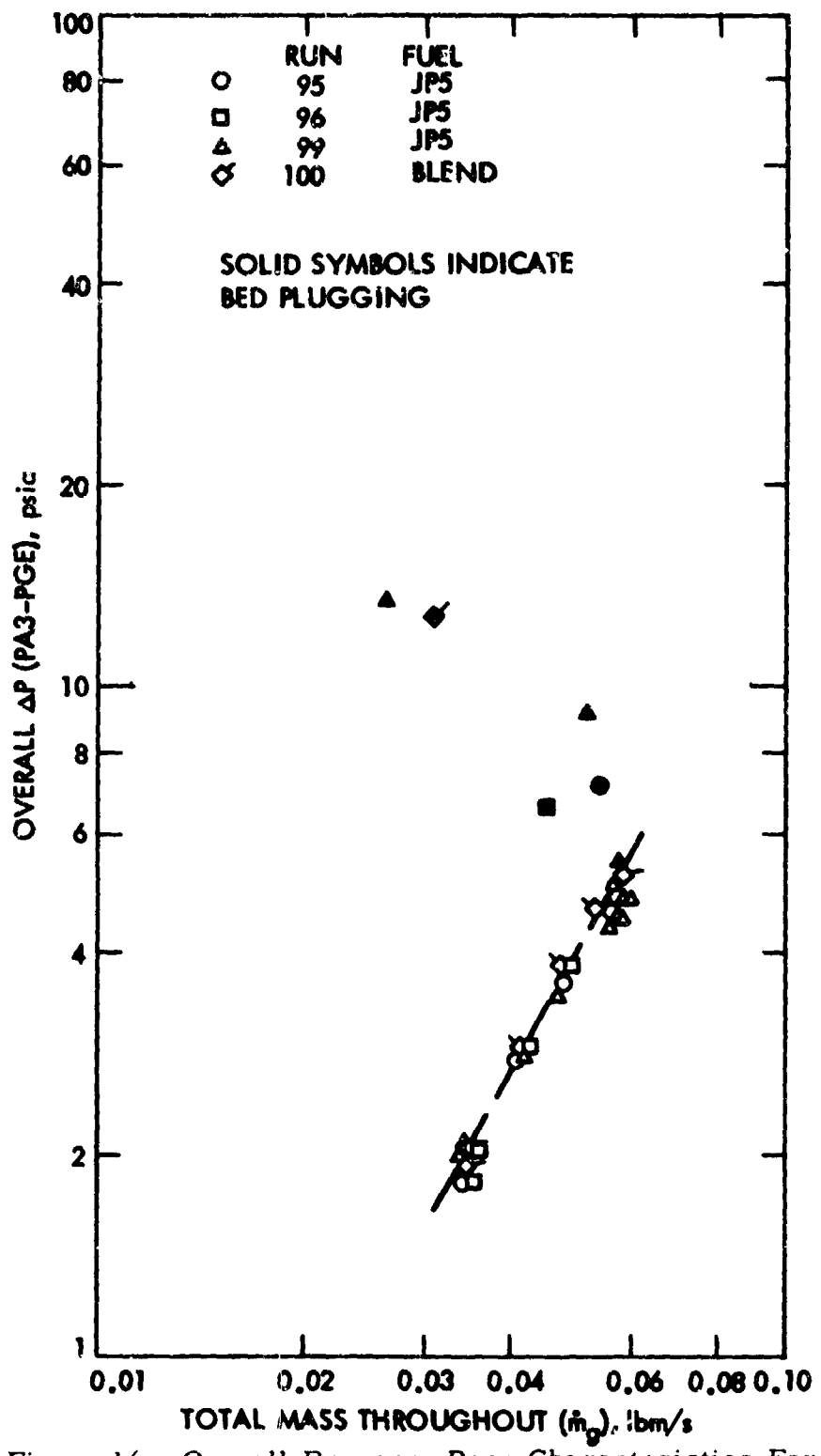


Figure 16. Overall Pressure Drop Characteristics For Generator L During Operation

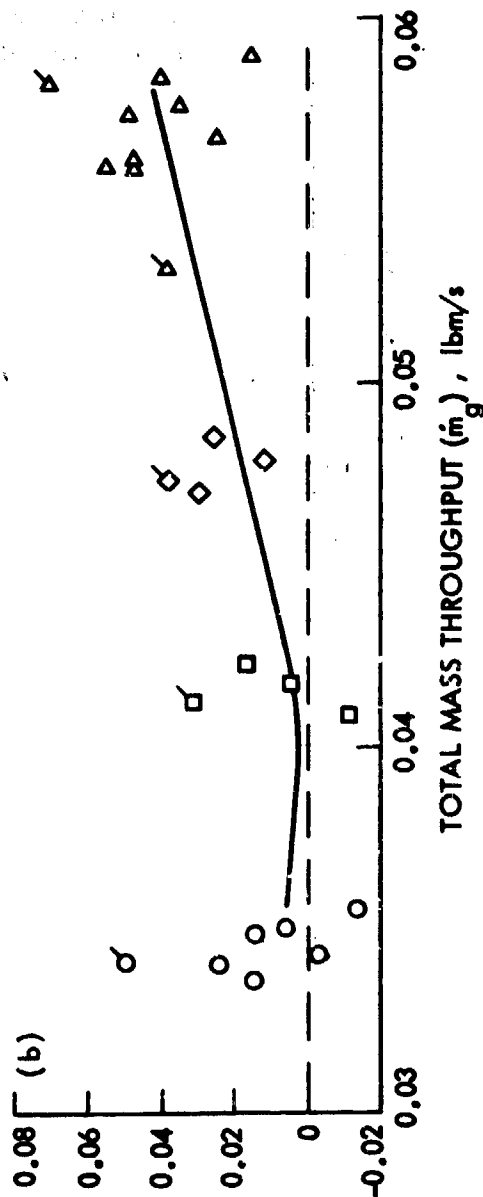
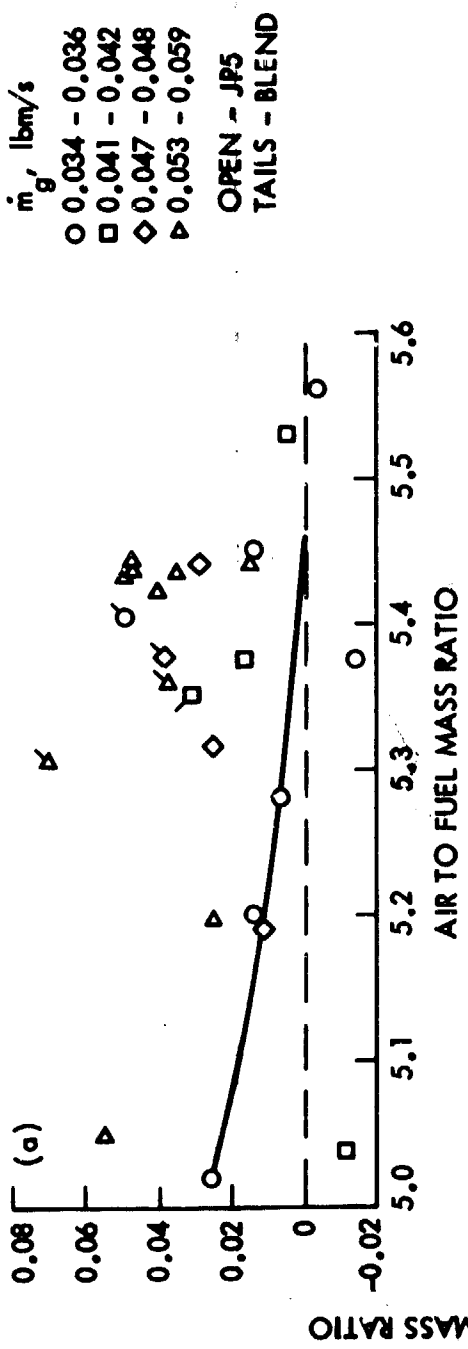


Figure 17. Calculated Solid Carbon Production for Generator L:
 (a) Versus Air to Fuel Ratio; (b) Versus Mass Throughput

TABLE 1. COMPARISON OF TWO-STAGE OPERATIONAL SCHEMES

<u>OPERATIONAL SCHEME</u>	<u>AIR SPLIT</u>	<u>FUEL SPLIT</u>	<u>ADVANTAGE</u>
1. All Fuel Through First Stage	Variable	Constant @ 100%	Greatest Benefit for Alternate Fuels
2. Constant Air Split to First Stage	Constant	Variable	Simpler Control
3. Parallel the Lean Limit Line	Variable	Variable	None
4. Constant Fuel Split to First Stage (< 100%)	Variable	Constant	None

TABLE 2. MEASUREMENT DESCRIPTION

<u>Measurement</u>	<u>Description</u>
PAI, PAIC, TAI, TAIC	Air supply line pressure and temperature
DPA	Air supply venturi pressure drop
PA2, TA2	Inlet plenum air pressure and temperature
PEX, TEX	Exhaust plenum gas pressure and temperature
DPO	PA2-PEX
PAG, TAG	Generator air supply line pressure and temperature
DPG	Generator air supply venturi pressure drop
PA3, PA4, TA3, TA4	Generator inlet air pressures and temperatures (before regenerative pre-heat)
PA5, TA5	Generator inlet air pressure and temperatures (after regenerative pre-heat)
PMI, TMI	Generator inlet mixture pressure and temperature
PBI, PB2	Static pressures in conical section of bed
PGE, TGE	Generator outlet pressure and temperature
TB1 thru TB7	Catalyst bed temperatures
PFL, TFL	Fuel supply line pressure and temperature
HZF1, HZF2	Fuel flow meters (alternate meters)

TABLE 2 (cont'd.)

<u>Measurement</u>	<u>Description</u>
TVH	Fuel vaporizer block temperature
PFV, TFV	Fuel vapor temperature (Vaporizer outlet)
PFJ, TFJ	Fuel vapor Temperature (at fuel injector)
PNI	Nitrogen purge gas pressure
PNW	Cooling water pressure (exhaust water spray)
TPG	Sample gas temperature at probe exit
TLG	Sample gas temperature at transfer line entrance
TSG	Sample gas temperature at transfer line exit

TABLE 3. TABULATED RESULTS

RUN-TEST POINT	OPERATING CONDITION							DRY MEASUREMENT				
	\dot{m} lbm/s	A/F	F/A EQUIV RATIO	PA3 psia	TA3 °F	TFJ °F	TM1 °F	PGE psia	H ₂ %V	CO %V	CO ₂ %V	CH ₄ %V
95-1	0.0340	5.022	2.944	49.67	236	543	558	47.81	23.03	24.38	1.03	0.53
-2	0.0349	5.201	2.843	49.92	261	544	561	47.87	22.23	24.01	1.26	0.56
-3	0.0409	5.039	2.934	51.34	292	554	583	48.55	23.52	25.16	0.80	0.50
-4	0.0479	5.190	2.849	52.78	313	561	602	49.17	22.27	24.53	1.09	0.26
-5	0.0567	5.196	2.845	56.52	334	558	604	51.67	22.05	24.23	1.25	0.20
-6	0.0559	5.049	2.929	59.60	338	543	576	54.93	22.13	23.78	1.36	0.38
-7	0.0537	5.292	2.795	61.47	339	530	595	54.37	21.64	23.16	1.67	0.52
96-1	0.0351	5.280	2.801	49.07	113	533	644	47.23	22.54	22.81	1.60	1.23
-2	0.0356	5.375	2.750	49.44	259	535	533	47.39	22.51	22.94	1.58	1.21
-3	0.0423	5.344	2.767	50.99	292	534	547	48.07	21.44	22.80	1.68	1.09
-4	0.0485	5.315	2.781	52.60	308	547	557	48.76	20.95	22.67	1.73	1.26
-5	0.0446	5.220	2.833	65.94	329	561	594	59.37	19.06	21.33	2.12	3.06
99-1	0.0336	5.452	2.712	54.36	245	538	526	52.37	20.82	22.93	1.93	0.61
-2	0.0344	5.562	2.658	54.30	261	542	548	52.21	20.77	23.21	1.75	0.53
-3	0.0417	5.531	2.674	56.18	284	554	569	53.37	20.57	23.64	1.57	0.29
-4	0.0470	5.441	2.718	57.39	302	558	586	53.92	21.28	23.67	1.58	0.14
-5	0.0574	5.431	2.723	59.69	319	557	586	54.91	19.87	23.29	1.75	0.10
-6	0.0563	5.435	2.732	59.77	322	547	572	54.73	20.08	23.26	1.76	0.13
-7	0.0559	5.444	2.717	61.88	328	499	534	57.57	20.41	23.09	1.70	0.17
-8	0.0584	5.422	2.727	64.71	334	479	530	60.23	21.09	23.11	1.65	0.20
-9	0.0576	5.435	2.721	64.55	335	471	537	60.01	20.79	23.18	1.62	0.32
-10	0.0589	5.438	2.719	68.13	339	465	517	63.31	21.04	23.86	1.24	0.33
-11	0.0574	5.450	2.713	67.89	341	485	549	62.38	21.12	22.64	1.72	1.12
-12	0.0516	5.411	2.733	77.41	344	536	574	68.36	20.41	22.50	1.79	0.92
-13	0.0262	5.409	2.734	79.02	338	525	593	65.57	21.15	22.59	1.63	1.07
100-1	0.0341	5.405	2.736	50.42	239	516	545	48.48	20.23	23.58	1.48	0.24
-2	0.0412	5.351	2.763	51.97	278	530	567	49.05	20.83	24.18	1.20	0.29
-3	0.0472	5.378	2.749	53.16	292	535	582	49.34	20.34	24.13	1.26	0.21
-4	0.0530	5.359	2.759	54.37	303	535	537	49.73	20.25	24.10	1.21	0.18
-5	0.0582	5.304	2.788	58.38	319	513	571	53.12	20.14	23.73	1.35	0.15
-6	0.0306	5.375	2.751	71.49	322	516	605	58.84	21.95	23.94	1.40	0.72

TABLE 3. TABULATED RESULTS (CONT)

RUN-TEST POINT	CALCULATED WET BASIS (EXCEPT C/F)									REMARKS
	H ₂ %V	CO%V	CO ₂ %V	CH ₄ %V	N ₂ %V	H ₂ O%V	C/F (by mass)	H/F (by mass)	H ₂ mass fract. in comb.	
95-1	22.88	24.22	1.02	0.53	50.69	0.66	0.0293	0.1225	0.0626	
-2	22.00	23.76	1.25	0.55	51.39	1.05	0.0166	0.1212	0.0614	
-3	23.57	25.21	0.80	0.50	50.12	-0.20	-0.0135	0.1266	0.0620	
-4	22.10	24.40	1.08	0.26	51.41	0.75	0.0121	0.1216	0.0605	
-5	21.83	23.98	1.24	0.20	51.74	1.02	0.0294	0.1203	0.0608	
-6	21.84	23.47	1.34	0.38	51.67	1.29	0.0642	0.1174	0.0619	
-7	21.29	22.78	1.64	0.51	52.15	1.63	0.0377	0.1190	0.0619	BED PLUGGED
96-1	22.20	22.47	1.53	1.21	51.05	1.49	0.0067	0.1239	0.0643	
-2	22.20	22.63	1.56	1.19	51.05	1.37	-0.0160	0.1258	0.0639	
-3	21.02	22.36	1.65	1.07	51.96	1.95	0.0195	0.1185	0.0615	
-4	20.49	22.18	1.69	1.23	52.23	2.18	0.0287	0.1150	0.0603	
-5	18.44	20.64	2.05	2.96	52.67	3.23	0.0334	0.1020	0.0562	BED PLUGGED
99-1	20.47	22.54	1.90	0.60	52.80	1.70	0.0147	0.1174	0.0602	
-2	20.40	22.79	1.72	0.52	52.78	1.79	-0.0027	0.1190	0.0595	JPS
-3	20.20	23.21	1.54	0.28	52.95	1.82	0.0049	0.1191	0.0582	
-4	19.88	23.20	1.55	0.14	53.26	1.97	0.0286	0.1138	0.0575	
-5	19.40	22.74	1.71	0.10	53.69	2.36	0.0481	0.1110	0.0573	
-6	19.63	22.73	1.72	0.13	53.53	2.26	0.0473	0.1123	0.0579	
-7	19.91	22.52	1.66	0.17	53.29	2.45	0.0469	0.1140	0.0592	
-8	20.63	22.60	1.61	0.20	52.76	2.20	0.0397	0.1178	0.0610	
-9	20.32	22.66	1.58	0.31	52.87	2.26	0.0346	0.1162	0.0598	
-10	20.61	23.37	1.21	0.32	52.43	2.05	0.0152	0.1179	0.0589	
-11	20.65	22.14	1.68	1.10	52.21	2.23	0.0096	0.1184	0.0610	BED PLUGGED
-12	19.85	21.89	1.74	0.89	52.90	2.73	0.0397	0.1131	0.0597	BED PLUGGED
-13	20.61	22.02	1.59	1.04	52.20	2.53	0.0249	0.1174	0.0613	BED PLUGGED
100-1	19.76	23.03	1.45	0.23	53.20	2.34	0.0498	0.1125	0.0575	
-2	20.46	23.74	1.18	0.28	52.54	1.80	0.0311	0.1155	0.0577	
-3	19.93	23.64	1.23	0.21	52.97	2.02	0.0380	0.1130	0.0566	
-4	19.81	23.58	1.18	0.18	53.09	2.15	0.0380	0.1120	0.0564	
-5	19.63	23.13	1.32	0.15	53.25	2.52	0.0698	0.1100	0.0570	
-6	21.76	23.73	1.39	0.71	51.54	0.87	-0.0101	0.1233	0.0606	BED PLUGGED